Presence of HLA-DR molecules and HLA-DRB1 mRNA in circulating CD4+ T cells

Revenfeld, Anne Louise Schacht; Steffensen, Rudi; Pugholm, Lotte Hatting; Jørgensen, Malene Møller; Stensballe, Allan; Varming, Kim

Published in:
Scandinavian Journal of Immunology

DOI (link to publication from Publisher):
10.1111/sji.12462

Publication date:
2016

Document Version
Publisher's PDF, also known as Version of record

doi: 10.1111/sji.12462

Presence of HLA-DR Molecules and *HLA-DRB1* mRNA in Circulating $CD4^+$ T Cells

A. L. S. Revenfeld*, R. Steffensen*, L. H. Pugholm*, M. M. Jørgensen*, A. Stensballe† & K. Varming*

*Department of Clinical Immunology, Aalborg University Hospital, Aalborg, Denmark;
†Laboratory for Medical Mass Spectrometry, Department of Health Science and Technology, Aalborg University, Aalborg, Denmark

Received 28 April 2016; Accepted in revised form 6 July 2016

Correspondence to: A. L. S. Revenfeld, Department of Clinical Immunology, Aalborg University Hospital, Urbansgade 32-36, DK-9000 Aalborg, Denmark. E-mail: anlor@rn.dk

Abstract

The human major histocompatibility complex class II isotype HLA-DR is currently used as an activation marker for T cells. However, whether an endogenous protein expression or a molecular acquisition accounts for the presence of HLA-DR on T cells remains undetermined and still controversial. To further characterize this phenomenon, we compared several aspects of the presence of the HLA-DR protein to the presence of associated mRNA (*HLA-DRB1*), focusing on human T cells from peripheral blood of healthy individuals. Using a flow cytometric approach, we determined that the HLA-DR observed on $CD4^+$ T cells was almost exclusively cell surface-associated, while for autologous $CD19^+$ B cells, the protein could be located in the plasma membrane as well as in the cytoplasm. Moreover, negligible expression levels of *HLA-DRB1* were found in $CD4^+$ T cells, using an *HLA-DRB1* allele-specific qPCR assay. Finally, the presence of HLA-DR was not confined to activated $CD4^+$ and $CD8^+$ T cells, as evaluated by the co-expression of CD25. The functional role of the HLA-DR molecule on T cells remains enigmatic; however, this study presents evidence of fundamental differences for the presence of HLA-DR on T cells from HLA-DR in the context of antigen-presenting cells, which is a well-known phenomenon. Although an inducible endogenous protein expression cannot be excluded for the T cells, our findings suggest that a re-evaluation of the HLA-DR as a T cells activation marker is warranted.

Introduction

It has been observed for more than four decades that T cells in peripheral blood can present MHC class II (MHCII) molecules on their outer surface and that the number of $MHCII^+$ T cells increases upon activation [1–4]. In line with this, one of the three human MHCII isotypes, called HLA-DR, is frequently used as a T cell activation marker along with other molecules, such as CD69 and CD25 [5–8]. Nonetheless, the functional role and significance of HLA-DR on human T cells is not fully determined and the unequivocal confirmation of an endogenous expression or a protein acquisition from other immune cells is absent. The constitutive expression of HLA-DR is limited to a few cell types, collectively called antigen-presenting cells (APCs) [9, 10]. These cells use HLA-DR to present antigenic peptides to $CD4^+$ T cells, and consequently, HLA-DR is involved in many facets of immune homoeostasis such as T cell activation, peripheral tolerance and induction of apoptosis [11].

Since the first observations of HLA-DR on T cells in the late 1970s, a number of studies have investigated aspects of the HLA-DR molecule in this particular context. Although still a subject of discussion, the general understanding is that the presence of this protein complex can be explained by either of two scenarios. The first involves an inducible *de novo*, endogenous protein synthesis, while the other encompasses a molecular acquisition from other immune cell types by currently unverified mechanisms. The studies supporting the former explanation have investigated several of the components involved in HLA-DR expression, transport and function, including lysosomal proteases [12], antigen presentation [13, 14] and engagement of CIITA [10, 12, 15], which is reported as the master regulator of *HLA-DR* expression [16–19]. Mouse T cells do not produce MHCII, which has been explained by a lack of CIITA expression [20]. However, even when CIITA is absent, MHCII expression is still observed for several cell types [21, 22]. The second phenomenon explaining HLA-DR on T cells is investigated in several other studies, demonstrating a transfer of a fully functional protein complex from APCs [23, 24]. In accordance with this, the MHCII observed on mouse T cells is a result of an acquisition from APCs [25–27]. In addition, a number of

SCANDINAVIAN JOURNAL OF Immunology AN INTERNATIONAL MONTHLY JOURNAL

studies have found that activated rat T cells can both synthesize and absorb MHCII molecules from adjacent cells [28–30]. The transfer of HLA-DR to human T cells has also been reported [31, 32], but a possible link between this acquisition and a potential endogenous expression of HLA-DR remains to be investigated.

Our study aimed to further explain the phenomenon of HLA-DR on human T cells in peripheral blood of healthy individuals. We addressed several aspects of the presence of the protein on T cells and correlated this with a transcript analysis of the corresponding mRNA. Moreover, the validity of HLA-DR as a T cell activation marker was investigated. The study was carried out to elucidate the physiological details of HLA-DR on T cells as well as to obtain novel information about a possible endogenous expression. Firstly, our results indicate that HLA-DR on $CD4^+$ T cells in peripheral blood could not be explained by a concurrent presence of an active protein synthesis. This points to important differences between the HLA-DR in the context of T cells as compared to APCs, which may be important, when deciphering the possible functions of HLA-DR-presenting T cells. In addition, we demonstrated that HLA-DR was not confined to activated T cells, thus suggesting to reassess the use of HLA-DR as an activation marker for T cells without any accompanying information.

Methods

Antibodies. The following conjugated antibodies were obtained from BD Biosciences (Mountain View, CA, USA): anti-CD3-PE (SK7), anti-CD3-PerCP (SP34-2), anti-CD4-APC-H7 (SK3), anti-CD4-PE (RPA-T4), anti-CD8-PerCP (SK1), anti-CD8-PerCP-Cy5.5 (SK1), anti-CD14-PE-Cy7 (M5E2), anti-CD19-APC (HIB19), anti-CD19-PE (4G7), anti-CD19-PerCP-Cy5.5 (SJ25C1), anti-CD25-FITC (2A3), anti-HLA-DR-FITC (G46-6), mouse IgG1-APC-H7 (X40), mouse IgG1-FITC (MOPC-21), mouse IgG2a-FITC (27-35), mouse IgG1-PE (MOPC-21), mouse IgG2a-PE (MOPC-173), mouse IgG1-PerCP (MOPC-21), mouse IgG1-PerCP-Cy5.5 (MOPC-21) and mouse IgG1-PE-Cy7 (MOPC-21). From BD Biosciences, the unconjugated anti-CD3 (HIT3a) was also acquired. Anti-CD45-FITC (T29/33), anti-HLA-DR-PE (AB3) and mouse IgG1-APC (DAK-GO1) were purchased from Dako A/S (Glostrup, Denmark). Anti-HLA-DR-Alexa Fluor (AF) 488 (L243), anti-HLA-DR-AF647 (L243), mouse IgG2a-AF488 (MOPC-173) and mouse IgG2a-AF647 (MOPC-173) were purchased from BioLegend (San Diego, CA, USA). Mouse IgG1-PerCP-Cy5.5 (P3.6.2.8.1) was obtained from eBioscience (San Diego CA, USA). The goat anti-mouse IgG-AF555 was purchased from Invitrogen (Life Technologies, Carlsbad, CA, USA).

Cells and isolation. Venous peripheral blood was obtained from healthy donors with known HLA types. Each blood donor had signed a written consent form, allowing for the use of his or her blood for research purposes. The procedure was approved by local ethics legislation. The blood was collected in heparinized tubes (Vacuette®, Lithium Heparin; Greiner Bio One, Frickenhausen, DE). Isolation of Peripheral blood mononuclear cells (PBMCs) was accomplished using Lymphoprep™ gradient centrifugation (Axis-Shield, Oslo, Norway). The PBMCs were either used directly after the isolation or stored at −140 °C in a storage medium [RPMI 1640 (Gibco, Life Technologies), 40% heat-inactivated foetal calf serum (FCS; Gibco), 10% DMSO (Merck Millipore, Darmstadt, Germany), 100 U/ml penicillin/10 μg/ml streptomycin (Ampliqon, Odense, Denmark)]. The $CD4^+$ T cells were isolated from PBMCs using the Dynabeads® CD4 Positive Selection kit (Invitrogen) according to the manufacturer's guidelines. As an additional purification step, any residual B cells were removed from the isolated $CD4^+$ T cells by positive selection, using Dynabeads® CD19 Pan B (Invitrogen). The purity of the isolated $CD4^+$ T cells was evaluated by staining with fluorochrome-conjugated antibodies with subsequent flow cytometric analysis. From the $CD4^+$ depleted PBMCs, $CD19^+$ B cells were isolated using the Dynabeads® Untouched™ Human B Cells kit (Invitrogen) according to the manufacturer's guidelines.

Detection of cell surface-associated and intracellular markers by flow cytometry. For the detection of cell surface-associated and intracellular HLA-DR, 1×10^6 PBMCs were stained with antibodies against CD3, CD19, HLA-DR (L243-AF488) or the corresponding isotype control antibodies (30 min, room temperature (RT)). Subsequently, 100 μl of fixation medium (reagent A) from FIX & PERM® Cell Fixation and Permeabilization Kit (Invitrogen) was added (15 min, RT). Following one wash with PBS (Gibco), a second antibody against HLA-DR (L243-AF647), or the corresponding isotype antibody, and 100 μl of permeabilization medium (reagent B) were added to the cells (20 min, RT). Finally, the cells were washed once with PBS prior to flow cytometric analysis. For the detection of cell surface-associated HLA-DR on $CD4^+$ and $CD8^+$ T cells, the procedure only included the primary surface staining, using antibodies against CD3, CD4, CD8, CD25 and HLA-DR (L243-AF647).

The flow cytometric analysis of stained cells was performed on a FACSCanto A using FACSDIVA™ software (version 6.1.3; BD Biosciences). Calibration and compensation settings for the cytometer were obtained each day using the 7-Color Setup Beads (BD Biosciences) and once a week with the FACSDIVA™ CS&T Research Beads (BD Biosciences). The analysis of the data was carried out with the FLOWJO software (version 10.0.7; FlowJo LLC, Ashland, OR, USA). Negative isotype controls were utilized to identify the positive events. The controls were either combined in a single tube or part of a 'fluorescence minus one' (FMO) tube [33]. The median fluorescence intensity (MFI) was the statistical value of choice.

Detection of cell surface-associated and intracellular HLA-DR by confocal microscopy. For all experiments, 1.5×10^5 isolated $CD4^+$ T cells or $CD19^+$ B cells were left to adhere to poly-L-lysine-coated slides (Sigma-Aldrich, St. Louis, MO, USA; 20 min, RT). The T cells were initially stained with anti-CD3 (HIT3a; 1:250; 45 min, RT), followed by incubation with secondary antibody (goat anti-mouse IgG-AF555; 1:200; 45 min, RT). Slides were washed three times in PBS and cells were fixed in 2% paraformaldehyde (PFA) (Sigma-Aldrich) (15 min, RT). Both T and B cells were then stained with anti-HLA-DR-AF488 (L243) (1:100; 45 min, RT). Slides were washed three times in PBS and cells were fixed in 2% PFA (15 min, RT) followed by another round of washing and permeabilization with permeabilization buffer [1% bovine serum albumin (BSA; Sigma-Aldrich), 0.1% saponin (Sigma-Aldrich), PBS; 8 min, RT]. To visualize cytosolic HLA-DR, cells were subsequently stained with anti-HLA-DR-AF647 (L243) (1:100 in permeabilization buffer; 45 min, RT). Slides were washed four times in PBS and mounted with mounting medium (Sigma-Aldrich). Images were captured with a Leica TCS SP5 confocal laser scanning microscope (Leica, Wetzlar, Germany) and a 100× oil immersion objective using the LAS AF software (Leica). All images were slightly adjusted for background fluorescence and signal intensity using IMAGEJ (version 1.48; NIH, Bethesda, MD, USA).

Total RNA extraction and cDNA synthesis. Total RNA was extracted from the isolated $CD4^+$ T cells and $CD19^+$ B cells using the TRIzol extraction method (Invitrogen). The A260/A280 ratio was determined using a NanoDrop 1000 Spectrophotometer (Thermo Scientific, Waltham, MA, USA). Total cDNA for the quantitative PCR (qPCR) was generated from 1 μg total RNA from all samples using a mixture of poly-T and random primers with SuperScript VILO cDNA Synthesis Kit (Invitrogen) at a temperature profile of 25 °C for 10 min, 42 °C for 60 min and 85 °C for 5 min according to the manufacturer's guidelines.

Quantitative PCR. PCR primers for amplification of 57–136-base pair gene-specific PCR products were used from conserved regions of the four studied genes (*HLA-DRB1*03*, *CD19*, *B2M*, and *GUSB*). Primers and FAM-labelled minor groove binder (MGB) TaqMan probes were used to detect the RNA expression level of the reference genes *B2M* and *GUSB* [34] and the target gene *HLA-DRB1*03* for which the *HLA-DRB1*03:01:01:01* mRNA sequence from the IMGT/HLA database was used as target sequence. Expression levels of *CD19* were detected using 20× probe assays mix (Life Technologies). The information about primer and probe sequences is given in Table 1. The qPCR assay was applied to evaluate the gene expression profiles of the four genes, and the data were analysed using the QuantStudio 12K Flex system (Life Technologies). The real-time PCR reactions were performed in a final volume of 25 μl, containing 1 μl cDNA solution, 12 μl Master Mix (TaqMan Universal PCR Master Mix; ABI, Darmstadt, Germany), 0.05 μM probe and 0.9 μM of forward and reverse primers. The PCR reaction for TaqMan gene expression assays contained 1 μl cDNA solution, 12 μl Master Mix and 1.25 μl TaqMan gene expression assay. Reactions were made up to a final volume of 25 μl with sterile water. All experiments were performed in triplicate and the real-time PCR protocol was as following: denaturation by a hot start at 95 °C for 10 min, followed by 50 cycles of a two-step program (denaturation at 95 °C for 15 s and annealing/extension at 60 °C for 1 min). For all the included gene targets, only the threshold cycle (Ct) values below 40 were included in the subsequent data analysis. Gene expression of the target gene was normalized to the mean Ct of *B2M* and *GUSB* applying the formula $2^{-\Delta Ct}$, where ΔCt = Ct target gene − Ct reference genes. The normalization, using the mean of the two reference genes, could be applied as target and reference genes were amplified with comparable efficiencies (data not shown).

Statistical analysis. The statistical analysis of data from both qPCR and flow cytometry experiments was performed using SIGMAPLOT (version 11; Systat Software Inc., San Jose, CA, USA). A paired or unpaired *t*-test was applied to test for differences between the groups of cells from the same individual or between two individuals, respectively. For non-normally distributed data, the corresponding nonparametric analysis was applied. Differences between groups were considered statistically significant, when $P < 0.05$. Unless otherwise specified, the data are presented as mean ± SEM.

Results

Identification and separation of HLA-DR on the cells surface and in the intracellular compartment of $CD3^+$ T cells

We initially wanted to investigate the cellular distribution of the HLA-DR antigen both on the cell surface/plasma membrane (HLA-DR mem) and in the intracellular space (HLA-DR IC) of $CD3^+$ T cells using flow cytometry. A two-step strategy was developed, including an initial staining of HLA-DR mem was followed by fixation, permeabilization of the plasma membrane and a secondary staining of HLA-DR IC. To separate the two separate HLA-DR localizations, two anti-HLA-DR antibodies of the same clone, but with different fluorophores conjugations, were applied (anti-HLA-DR mem AF488; anti-HLA-DR IC AF647). The distribution of HLA-DR mem and HLA-DR IC in $CD3^+$ T cells was compared to the distribution in $CD19^+$ B cells, as the HLA-DR expression pattern in this APC is well characterized. Our flow cytometric assay necessitated a number of analytical and experimental controls to ensure the validity of such an approach.

Table 1 Primer and probe sequences, assay id and amplicon size for the genes analysed by qPCR.

Gene	Primers	FAM-labelled MBG probe	Amplicon size	Exon boundary
*HLA-DRB1*03*	F: 5′-CACCTATTGCAGACACAA-3′ R: 5′-AACCACTCACAGAACAGA-3′	5′-ACCTTAGGATGGACTCGC-3′	136	2–3
B2M	F: 5′-GAGTATGCCTGCCGTGTG-3′ R: 5′-AATCCAAATGCGGCATCT-3′	5′-CCTCCATGATGCTGCTTACATGTCTC-3′	109	3
GUSB	F: 5′-GAAAATATGTGGTTGGAGAGCTCATT-3′ R: 5′-CCGAGTGAAGATCCCCTTTTTA-3′	5′-CCAGCACTCTCGTCGGTGACTGTTCA-3′	100	11–12
CD19	Hs01047410_g1		57	1–2

F, forward; R, reverse.
The specificity of the *HLA-DRB1*03* assay is located in the forward primer. For *B2M*, the forward primer is located in exon 2 and reverse primer in exon 4.

For the analysis, the gating control called the FMO [33] was applied to identify the HLA-DR mem and HLA-DR IC-positive events (Fig. 1). This approach is very useful for resolving weakly stained cells in multicolour panels in flow cytometry analyses [35, 36]. It also aids in placing a gate for a marker, which displays a continuous expression pattern, as is the case for HLA-DR on T cells. The applied FMO included a tube containing all markers and replacing the HLA-DR antibody of interest with an isotype control antibody. In this way, the HLA-DR single and double positive events could be determined, as exemplified in Fig. 1.

To verify the experimental setup, in which the plasma membrane-associated HLA-DR mem could be separated from the intracellular HLA-DR IC, it was essential to demonstrate and validate that a saturation of HLA-DR mem was obtained with the initial staining step. Hence, a saturation control was included in which all antibodies and staining conditions were applied, only omitting the permeabilization agent. Consequently, the HLA-DR IC signal should be absent in this sample if both the HLA-DR mem staining had saturated all cell surface-associated HLA-DR and no HLA-DR IC antibody entered the cell (Fig. 2). Initially, the optimal amount of applied anti-HLA-DR mem (L243-AF488) was determined with an 8-point titration experiment (0.025–4 μg; data not shown). The optimal amount (1 μg) was applied for staining with both anti-HLA-DR antibodies. For the saturation control experiments, it was observed as a general feature that a small HLA-DR IC signal could be detected in the saturation control for both the $CD3^+$ HLA-DR mem^+ T cells and $CD19^+$ HLA-DR mem^+ B cells (Fig. 2B). However, for the $CD3^+$ T cells, this signal never surpassed the HLA-DR IC signal from the fully stained sample. Similar observations were made for the $CD19^+$ B cells. A doubling of the applied amount of both HLA-DR antibodies did not increase or decrease the recorded intensities and cellular distributions of these markers (data not shown).

As a final investigation, the antibody staining procedure applied in the flow cytometric analysis was tested in a confocal microscopy setting. The purpose of this qualitative analysis was to visualize the separation of the fluorescence signals obtained, when targeting HLA-DR mem and HLA-DR IC with two different anti-HLA-DR antibodies. In contrast to the flow cytometric analysis, in which $CD3^+$ T cells and $CD19^+$ B cells from peripheral blood were the target cells, isolated $CD4^+$ T cells and $CD19^+$ B cells were used for the confocal microscopy investigation. With these cells, it was shown that $CD4^+$ T cells presenting HLA-DR mem could be identified (Figure S1A, top panel). In contrast, $CD4^+$ T cells presenting both HLA-DR mem and HLA-DR IC were almost absent (Figure S1B). To ensure that the observed HLA-DR signals in the $CD4^+$ T cell population were not due to contaminating APCs, such as monocytes, the identification of these T cells included a CD3 antibody. For the $CD19^+$ B cells, the HLA-DR proteins were present in both the plasma membrane and intracellular compartment of the entire cell population (Figure S1A, bottom panel). The purity of the isolated $CD4^+$ T cells and $CD19^+$ B cells was $97.6 \pm 2.2\%$ and $96.6 \pm 0.4\%$, respectively, as determined by flow cytometry ($n = 2$; data not shown).

Dimorphic distribution of HLA-DR in the plasma membrane and intracellular compartment of $CD3^+$ T cells and $CD19^+$ B cells

Based on the abovementioned staining and gating strategy and experimental approach, we identified the fraction of $CD3^+$ T cells from peripheral blood in which HLA-DR could be found in either the plasma membrane or the intracellular compartment or in both. An identical procedure was carried out for autologous $CD19^+$ B cells, to ensure a positive reference. The presence of HLA-DR mem on $CD3^+$ T cells and $CD19^+$ B cells differed significantly in terms of the percent-wise distribution. For the T cells, $18.2 \pm 4.2\%$ $CD3^+$ HLA-DR mem^+ cells were identified, while this number was 98.8 ± 0.5 for the B cells ($n = 10$). The associated P-value was 0.002. Moreover, the corresponding median fluorescence intensity (MFI) values were also markedly different with a nearly 14 times greater MFI

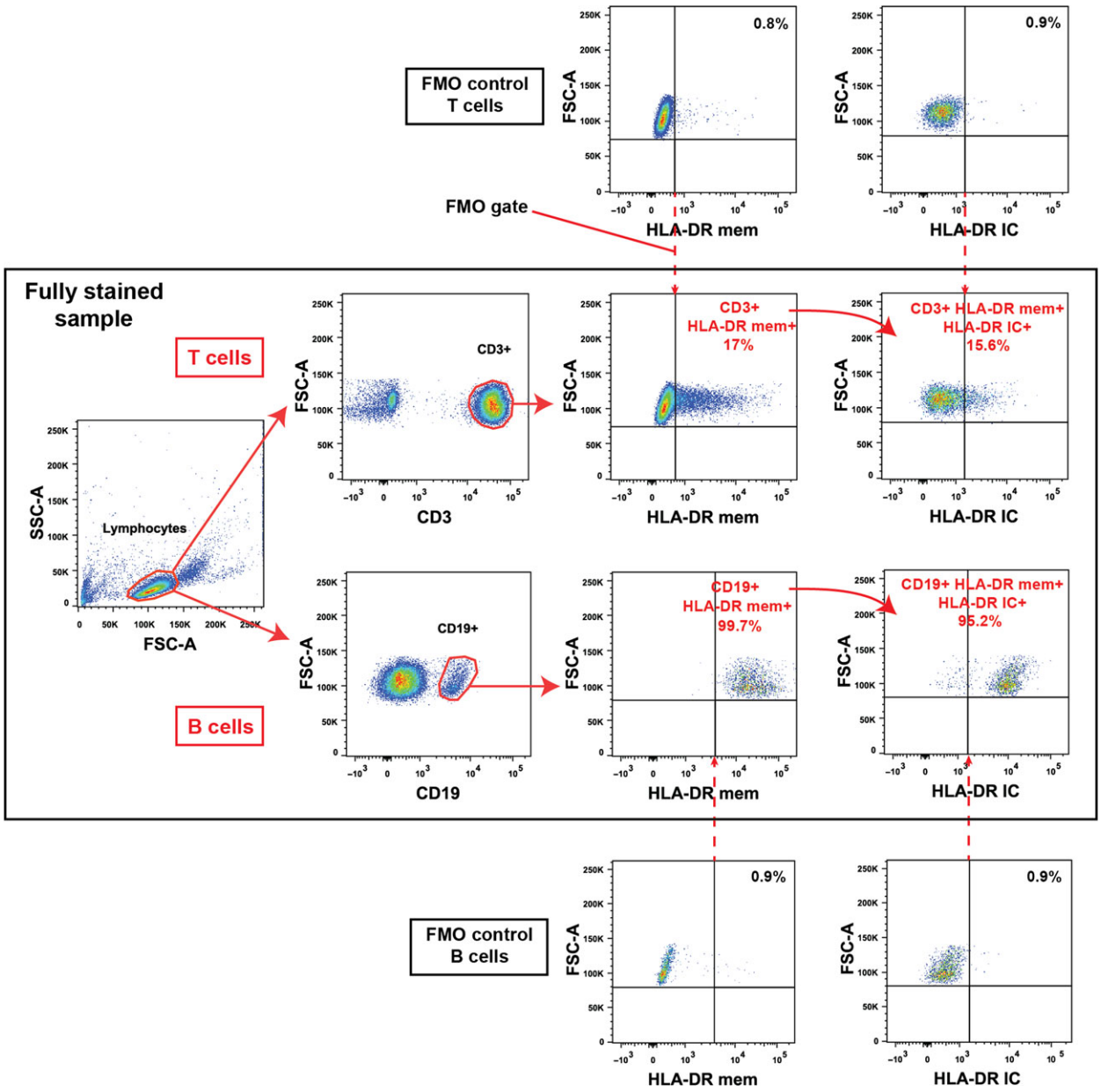

Figure 1 Improved flow cytometric gating strategy identifies HLA-DR in the plasma membrane and intracellular compartment of $CD3^+$ T cells and $CD19^+$ B cells. Initially, the lymphocyte population was gated in a forward scatter/side scatter plot. From the lymphocytes, the $CD3^+$ T cells and $CD19^+$ B cells were subsequently gated. Subsequently, the $CD3^+$ HLA-DR mem^+ (17%) and $CD19^+$ HLA-DR mem^+ (99.7%) populations were identified with pre-defined gates set using the fluorescence minus one (FMO) control for HLA-DR mem. In the last step, it was determined, which HLA-DR mem^+ cells also carried the HLA-DR protein intracellularly. For this purpose, gates set with the FMO controls were used, identifying the double positive $CD3^+$ HLA-DR mem^+ HLA-DR IC^+ (15.6%) and $CD19^+$ HLA-DR mem^+ HLA-DR IC^+ (95.2%) populations. For all the FMO controls, the threshold was set so that a maximum of 1% of the events fell into the double positive quadrant. The plots are from one donor as a representative example of the 10 included donors.

value detected for the $CD19^+$ B cells (23,047 ± 2059) than the equivalent value for the $CD3^+$ T cells (1662 ± 138). For the $CD3^+$ T cells, 17.9 ± 2.5% of the $CD3^+$ HLA-DR mem^+ cells also contained HLA-DR IC. This was significantly higher for the $CD19^+$ B cells (96.9 ± 0.9; $P < 0.001$). Here, the MFI for HLA-DR IC in the $CD19^+$ B cells (9227 ± 596) was approximately 5.5-fold higher compared to the MFI for the $CD3^+$ T cells (1748 ± 152). Finally, the analysis identified 3.0 ± 0.7% $CD3^+$ HLA-DR IC^+ and these were all HLA-DR mem^+ (Fig. 3A). The corresponding $CD19^+$ HLA-DR IC^+ B cells amounted to 95.9 ± 1.2% and these were also all HLA-DR mem^+. To investigate whether the T cells, which presented cell surface-associated HLA-DR to the greatest extent, also carried the largest amount of HLA-DR IC, a correlation for HLA-DR in the two compartments was

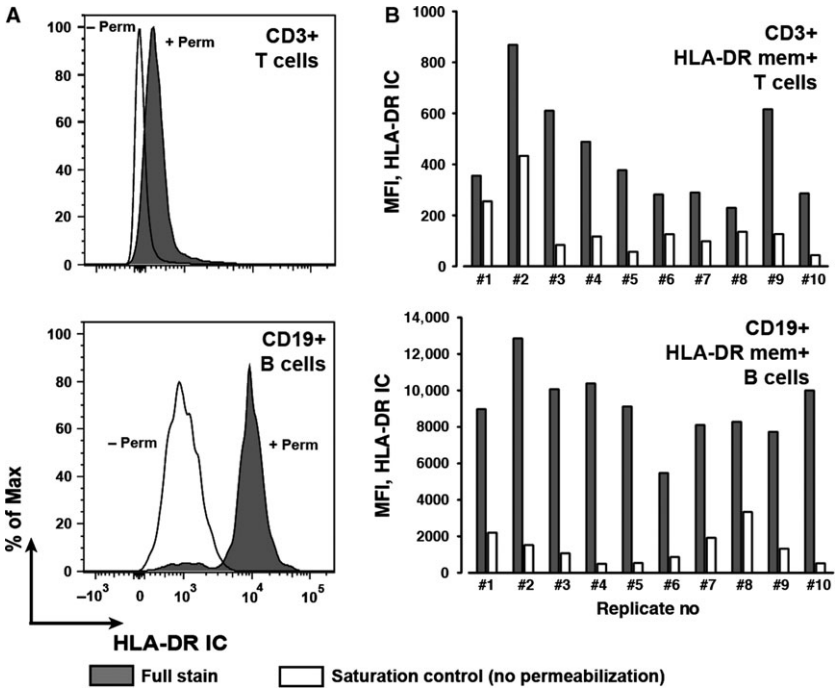

Figure 2 Comparison of HLA-DR IC signal in CD3+ T and CD19+ B cells with/without permeabilization of the outer plasma membrane. To test for saturation of cell surface HLA-DR (HLA-DR mem) with the initially applied anti-HLA-DR antibody, a saturation control was made for all the included donors. For the control, the entire staining setup was applied, only omitting the permeabilization agent. Subsequently, the gating strategy displayed in Fig. 1 was applied to identify the CD3+ HLA-DR mem+ T cells and CD19+ HLA-DR mem+ B cells. (A) The histograms show the HLA-DR IC signals for the HLA-DR mem+ cells for the fully stained sample and the saturation control. The histograms are a representative example of the 10 donors included in the study. (B) For all the 10 donors, there was a detectable HLA-DR IC signal present in the saturation control for both the CD3+ T cells and the CD19+ B cells. However, this signal was always lower than the specific HLA-DR IC signal detected in the fully stained sample.

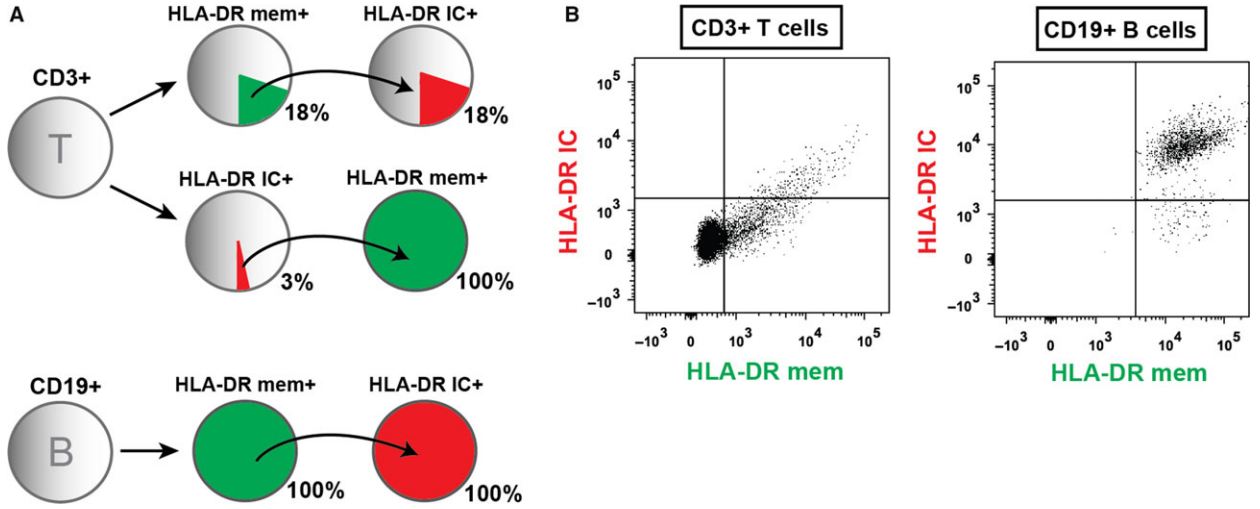

Figure 3 Correlation between HLA-DR mem and HLA-DR IC in CD3+ T cells and CD19+ B cells. (A) The distribution of HLA-DR mem and HLA-DR IC determined by flow cytometry for CD3+ T cells and CD19+ B cells. The circle charts visualize the obtained results (n = 10). (B) The gating strategy presented in Fig. 1 was employed to identify the HLA-DR mem+ and HLA-DR IC+ CD3+ T cells and CD19+ B cells in the presented dot plots. These plots were made to visualize a possible correlation between HLA-DR in the two cellular compartments. Both dot plots are representative examples of the included donors (n = 10).

made. This revealed that a positive correlation between these two proteins existed, both for CD3+ T cells and CD19+ B cells (Fig. 3B).

Relative contribution of CD4+ and CD8+ T cells to CD3+ HLA-DR mem+ T cell subset

In addition to the results about the presence of HLA-DR mem and HLA-DR IC for CD3+ T cells, it was investigated to which extent CD4+ and CD8+ T cells each contribute to the CD3+ HLA-DR mem+ subset. Accordingly, CD3+ CD4+ HLA-DR mem+ and CD3+ CD8+ HLA-DR mem+ T cells (hereafter referred to as CD4+ HLA-DR mem+ and CD8+ HLA-DR mem+ T cells) were identified in a flow cytometric analysis of PBMCs. The presence of HLA-DR mem was evaluated for these cells (Fig. 4A, top panel) using the FMO approach described in Fig. 1. This resulted in the detection of 8.9 ± 1.6% CD4+

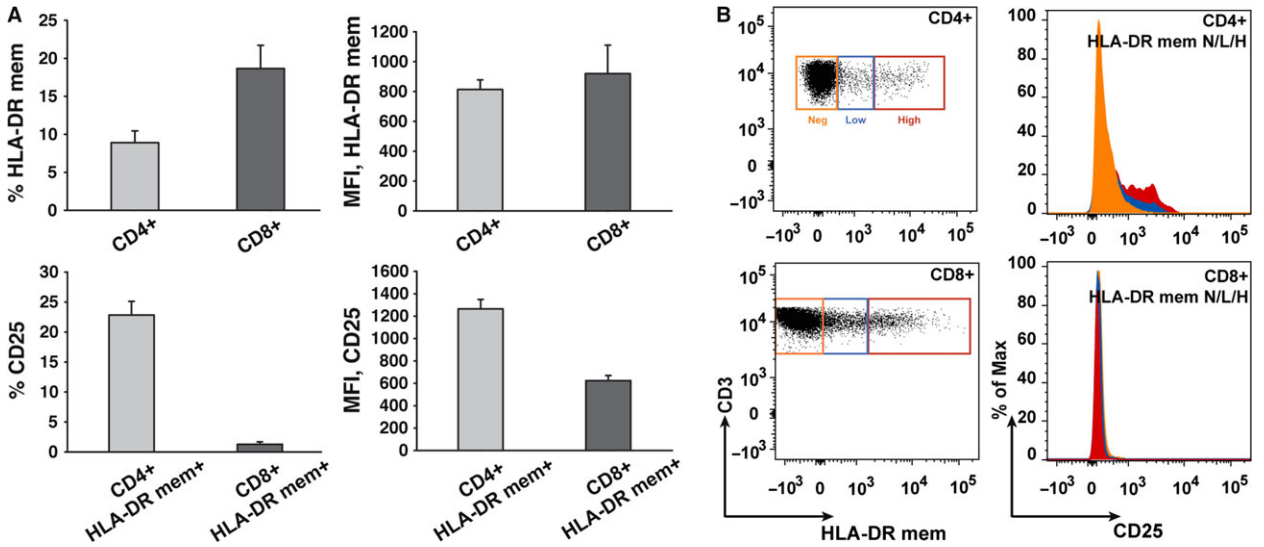

Figure 4 Contribution of $CD4^+$ and $CD8^+$ T cells to the $CD3^+$ HLA-DR mem^+ T cell population. The relative contribution of $CD4^+$ and $CD8^+$ T cells to the $CD3^+$ HLA-DR mem^+ T cell population was investigated by staining PBMCs with antibodies against CD3, CD4, CD8, CD25, and HLA-DR mem. (A) Using the gating strategy described in Fig. 1, the HLA-DR mem-presenting $CD4^+$ and $CD8^+$ T cells were identified (top panel, left). In addition, the corresponding median fluorescence intensity (MFI) values for HLA-DR mem were obtained (top panel, right). Subsequently, the percent-wise co-expression of CD25 was determined for the $CD3^+$ $CD4^+$ HLA-DR mem^+ and $CD3^+$ $CD8^+$ HLA-DR mem^+ cells (bottom panel, left) along with the corresponding MFI (bottom panel, right). Data are presented as the mean±SEM ($n = 6$). (B) The highest degree of CD25 expression was observed for the $CD4^+$ T cells, which presented the most HLA-DR mem (top panel). In contrast, CD25 was found to the greatest extent of the $CD8^+$ T cells presenting no HLA-DR mem (bottom panel).

HLA-DR mem^+ T cells and 18.7 ± 3.1% $CD8^+$ HLA-DR mem^+ T cells ($n = 6$). As the CD4/CD8 ratio in peripheral blood is approximately two for adults [37, 38], the $CD4^+$ and $CD8^+$ T cells each contributed roughly equally to the entire $CD3^+$ HLA-DR mem^+ T cell population.

To further characterize the HLA-DR mem-presenting $CD4^+$ and $CD8^+$ T cells, the co-expression of another T cell activation marker, CD25, was also investigated for these cells. Of the $CD4^+$ HLA-DR mem^+, 22.8 ± 2.3% co-expressed CD25 (Fig. 4A, bottom panel). Additionally, CD25 was enriched in the $CD4^+$ HLA-DR mem^+ population, when compared to the corresponding $CD4^+$ HLA-DR mem^- population, for which the expression of CD25 was 12.7 ± 1.2% (Fig. 4B). In contrast, the CD25 expression was greatest in the HLA-DR mem^- subset of the $CD8^+$ T cells (3.5 ± 0.8%) as compared to the $CD8^+$ HLA-DR mem^+ T cells (1.3% ± 0.3).

Contrasting expression profiles of HLA-DRB1 mRNA in $CD4^+$ T cells and $CD19^+$ B cells

To link the presence of the HLA-DR protein in T cells to its transcription, an investigation of the *HLA-DRB1* mRNA expression by qPCR was performed. The assay targeted a specific allele of the most prevalently expressed beta subunit of the heterodimeric HLA-DR protein, namely the beta 1 (B1) chain. For the specific allele, we chose *HLA-DRB1*03* (Table 1), which is a part of the DR52 haplotype (*HLA-DRB1*03, *11, *12, *13 and *14)* [39]. The amount of *HLA-DRB1* transcripts in this haplotype is the most abundant, compared to other haplotypes [40], making it a plentiful and advantageous target. To ensure that only the desired target was amplified, the *HLA-DRB1*03*-specific assay was initially tested on a panel of PBMCs from 13 individuals with *HLA-DRB1* alleles representative of the major DR haplotypes [39] (data not shown). Accordingly, the *HLA-DRB1*03*-positive individuals were selected, when they had either the homozygous *HLA-DRB1*03* genotype or the heterozygous *HLA-DRB1*03/*15* genotype. For the *HLA-DRB1*03*-negative samples, individuals with either the homozygous *HLA-DRB1*15* genotype or the heterozygous *HLA-DRB1*01/*07* were selected.

Subsequently, the expression pattern of *HLA-DRB1*03* was determined for human, isolated $CD4^+$ T cells and $CD19^+$ B cells from peripheral blood. As for the flow cytometric analysis of HLA-DR mem and HLA-DR IC, the $CD19^+$ B cells were included as a positive control. The qPCR analysis was performed with cells from individuals with either a positive or a negative *HLA-DRB1*03* genotype, as indicated on the section above. The results of the expression analysis are displayed in Fig. 5A. The difference, which was observed between $CD4^+$ T cells and $CD19^+$ B cells with an *HLA-DRB1*03*-positive genotype, corresponded to a 240-fold higher transcript quantity in the B cells. No detectable signal was obtained for the

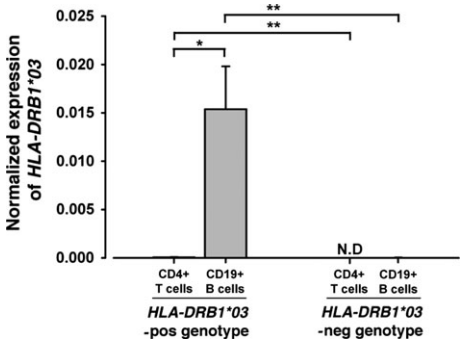

Figure 5 Quantifying mRNA from target genes by qPCR. The expression of HLA-DRB1*03 mRNA was investigated in isolated $CD4^+$ T cells and $CD19^+$ B cells from donors with an HLA-DRB1*03 positive or negative genotype ($n = 5$ for each genotype). The expression of the target gene was normalized to the mean of two reference genes (B2M and GUSB). Data is presented as mean±SEM. Statistical significant differences are indicated with p-values; *p<0.05; **p<0.01.

$CD4^+$ T cells with an *HLA-DRB1*03*-negative genotype. In contrast, two of the five corresponding $CD19^+$ B cell samples produced a detectable signal, yielding normalized expression values in a similar range as those for the $CD4^+$ T cells from the *HLA-DRB1*03*-positive individuals. The corresponding Ct values were 37.18 ± 0.17 ($n = 2$) and 36.20 ± 0.52 ($n = 5$), respectively.

As determined by flow cytometry, the purity of the isolated $CD4^+$ T cells was 98.8 ± 0.37% ($n = 10$; data not shown). Moreover, the presence of any cellular contamination, which could contribute to the minimally detected mRNA signal in the $CD4^+$ T cells from the *HLA-DRB1*03*-positive individuals, was also investigated. First, the amount of mRNA for *CD19* was evaluated by qPCR. This B cell differentiation marker was included as B cells constitute the largest *HLA-DRB1*-expressing population in PBMCs, thus encompassing the greatest source of a possible cellular contamination. The *CD19* gene transcripts were approximately 1500 times more abundant in the $CD19^+$ B cell samples compared to the $CD4^+$ T cell samples, regardless of *HLA-DRB1*03* genotype (data not shown). Secondly, the presence of $CD14^+$ monocytes was also assessed by flow cytometry. For the investigated samples, 0.97 ± 0.10% $CD4^+$ $CD14^+$ cells could be detected ($n = 8$ of the 10 included for qPCR analysis; all the *HLA-DRB1*01*-positive donors were included).

Discussion

The presence of HLA-DR antigens on T cells has been observed for more than four decades. The expression pattern and functionality of HLA-DR is well described for APCs but in the context of T cells, many unidentified aspects still remain.

With the use of a stringent staining and gating strategy for flow cytometry, this study investigated the distribution of HLA-DR in the cellular membrane (HLA-DR mem) and intracellular compartment (HLA-DR IC) of human $CD3^+$ T cells from peripheral blood. As a positive reference, this distribution was compared to that of autologous $CD19^+$ B cells. We hypothesized that if the cell of question contained the functional protein in both the membrane and intracellular compartment, it was likely that an endogenous protein expression existed.

The flow cytometric analysis identified that approximately 18% of $CD3^+$ T cells from peripheral blood contained HLA-DR mem (Fig. 3A). Other studies, which investigate HLA-DR on T cells, generally report a smaller amount of HLA-DR mem^+ T cells. However, these reports range widely from less than 5% [37, 38] to approximately 10% [7], but also above 15% [41, 42]. Using FMO controls [43] to set less user-biased positive gates than previously performed, the estimation of HLA-DR^+ cells is consequently more accurate. The identification of a uniformly HLA-DR mem-expressing, autologous B cell population validated the applied strategy. For future identification of HLA-DR on T cells, this strategy could therefore prove very useful. Only a few per cent of all $CD3^+$ T cells in peripheral blood contained HLA-DR IC (Fig. 3A), and we believe that this fraction of $CD3^+$ T cells has not previously been evaluated. Interestingly, a positive correlation between HLA-DR mem and HLA-DR IC was observed for both $CD3^+$ T cells and $CD19^+$ B cells (Fig. 3B). However, not all $CD3^+$ HLA-DR mem^+ T cells were also HLA-DR IC^+ (Fig. 3A), which might be expected if an active protein synthesis was present. Regardless, the results obtained from the presented experiments point to significant differences for HLA-DR in the context of T cells and APCs of which the latter comprise a well-documented constitutive expression of this protein.

To further investigate the link between the presence of the HLA-DR protein on T cells to an endogenous expression, a transcriptional analysis of *HLA-DRB1* was performed, using an allele-specific qPCR assay, targeting the *HLA-DRB1*03* allele in isolated $CD4^+$ T cells and $CD19^+$ B cells. By choosing to target only one allele, it was intended to circumvent the issues associated with the extensive homology of the *HLA-DR* genes, thus providing unambiguous expression results. With the qPCR of *HLA-DRB1*03* presented here, only minimal amounts of transcripts could be detected in the $CD4^+$ T cells from *HLA-DRB1*03*-positive individuals, while autologous $CD19^+$ B cells clearly possessed an active gene transcription of *HLA-DRB1* (Fig. 5). The marginally positive signals obtained for the T cells were very close to the expected and inevitable non-specificity of the assay. It was not expected that the *HLA-DRB1*03*-negative $CD4^+$ T cells could yield a similar non-specific signal, as these cells would not produce B cell-comparable amounts of *HLA-DRB1* transcripts, given the existence of such a production in the $CD4^+$ T cells. Moreover, a cellular

contamination with approximately 1% of residual monocytes, known to express both HLA-DR [44] and CD4 [45], could very likely have contributed to the *HLA-DRB1*03* mRNA in the relevant $CD4^+$ T cell samples. In total, this suggests that the signal detected in the $CD4^+$ T cells with an *HLA-DRB1*03*-positive genotype could be non-specific or ascribed to a possible cellular contamination from APCs.

When correlated with the flow cytometric analysis of HLA-DR, the results from the qPCR assay signify that the presence of HLA-DR on the surface of a rather constant-sized population of circulating $CD4^+$ T cells in healthy individuals cannot be explained by a concomitant presence of an active gene expression. Even if the specific mRNA may have been partially degraded in the HLA-DR-presenting $CD4^+$ T cells, it can be still be reasonably expected that these cells would give rise to a detectable *HLA-DRB1* mRNA signal, if an expression was present, as they constituted roughly 9% of the investigated cells. However, the results do not exclude the possibility that an inducible, endogenous expression of HLA-DR is present in these T cells. They also do not exclude the possibility that mRNA levels and protein expression of HLA-DR do not correlate in the investigated T cells. Nevertheless, this study showed tendencies for circulating HLA-DR-presenting $CD4^+$ T cells in healthy individuals, thus describing the physiological details of HLA-DR on T cells. These characteristics may be different for $CD4^+$ HLA-DR mem^+ T cells found in others tissues, such as in the lymph nodes, where elevated levels of HLA-DR-presenting T cells have been observed [41]. To support these theories and to fully appreciate the presence and dynamics of HLA-DR on human T cells, further analyses are required. These could include activated $CD4^+$ T cells in lymphoid tissue, such as the palatine tonsils, or in individuals with constantly activated T cells, such as HIV-infected patients [46]. Concomitant analysis of CIITA expression would also further complement the HLA-DR analysis.

In classical terms, HLA-DR has been used to identify activated T cells [5–8]. Our analyses revealed that $CD4^+$ and $CD8^+$ T cells each account for approximately 50% of the entire $CD3^+$ HLA-DR mem^+ subset in peripheral blood. However, the presence of HLA-DR mem was seemingly not confined to activated $CD4^+$ and $CD8^+$ T cells, as evaluated by a co-expression CD25 (Fig. 4A). In effect, the expression of CD25 on the $CD8^+$ HLA-DR mem^+ T cells was minimal, while the co-expression of the two proteins was found to correlate to a higher degree for the $CD4^+$ T cells (Fig. 4B). Although both $CD4^+$ HLA-DR mem^+ [4, 47] and $CD8^+$ HLA-DR mem^+ T cells [48] found in peripheral blood have been associated with regulatory functions, the difference in the expression of CD25 presented in this study could indicate distinct functionalities of these two cellular subsets. However, further investigations are required to substantiate this hypothesis.

In terms of functionality, HLA-DR on T cells has mainly been associated with immunosuppressive signals, inducing either apoptosis or anergy in activated T cells [4, 49, 50]. However, reports about T cell activation can also be found [26, 32]. Nonetheless, it seems that the function of HLA-DR in APCs cannot simply be extrapolated to T cells, which is based on a number of observations from this and other studies. In the current study, clear differences were demonstrated for the presence of HLA-DR both at the protein and transcript level, when comparing $CD4^+$ T cells to $CD19^+$ B cells. Others describe how T cell–T cell and T cell–APC interactions have significantly different effects on the responder T cells. Although TCR involvement, and consequently also HLA-DR, and co-stimulatory molecules are present for both types of cellular interaction [50], the resulting cytokine production (IL-2 and IL-4) and Ca^{2+} influx differ [49, 51, 52]. Moreover, most T cell–T cell interactions seemingly result in the induction of anergy, further underlining these differences [50]. In relation to key features of APCs, the mechanism for antigen acquisition remains unidentified for T cells [12], while other studies have investigated other requirements of antigen presentation in these cells, including HLA-DM, CLIP and proteolytic enzymes [12, 50]. Finally, the expression of essential co-stimulatory molecules, including CD80 and CD86, has been investigated. While some report an endogenous expression by T cells [50], others demonstrate an acquisition of functional molecules from APCs [32, 53, 54]. One of these studies demonstrated a simultaneous acquisition of HLA-DR by $CD4^+$ T cells in a contact-dependent manner [32], but also a contact-independent transfer of HLA-DR has been shown [27]. It has been recognized that immune cells are particularly prone to engage in such molecular exchange, bestowing new functional phenotypes on the recipient cells [55–61]. This challenges the classical subdivision of immune cells, which is based on such functional phenotypes, and also expands the regulatory mechanisms of the immune system. In relation to HLA-DR, many studies have used allogeneic stimulator cells to activate T cells, as part of a mixed lymphocyte culture, thereby inducing the presence of HLA-DR. However, if acquisition of HLA-DR and other molecules can occur in such a cell culture, it will have a major impact on future study design and interpretation of data and possibly also explain some of the contradictory results reported about HLA-DR in T cells to date [50].

In this study, we further elucidated the presence of HLA-DR on human T cells. To the best of our knowledge, no study has to date investigated the direct *HLA-DRB1* expression in human $CD4^+$ T and $CD19^+$ B cells from peripheral blood and correlated it to the concurrent presence of HLA-DR antigens in the plasma membrane and intracellular compartment. Using this approach, we were able to document fundamental differences between

HLA-DR in connection with T cells and APCs in healthy individuals, both at the protein and the transcriptional level. Moreover, we demonstrated that HLA-DR is not limited to activated T cells, thus challenging the use of HLA-DR as a T cell activation marker without supplementary information. Collectively, this study adds more layers to the understanding of the presence of HLA-DR on T cells. With a possible connection between HLA-DR and regulatory functions of T cells, questions of a possibly significant role of HLA-DR for T cells emerge. It also underlines the immense complexity of one of the most important molecules for the antigen specificity and function of the adaptive immune system.

Acknowledgment

The authors thankfully acknowledge Dr. Svend Birkelund, Aalborg University, for his invaluable help with the confocal microscopy experiments. We also thank technician Anne Elbæk, Department of Clinical Immunology, Aalborg University Hospital, Denmark, for excellent technical assistance.

Competing interest

The authors declare that they have no competing interests.

Author contributions

ALSR designed, performed and analysed data from the flow cytometric analyses, qPCR and confocal microscopy experiments and also drafted the manuscript. RS designed and performed the qPCR experiments and edited the manuscript. LHP performed the experimental procedures and the data analysis of the confocal microscopy and edited the manuscript. AS, MMJ and KV contributed to the study design, supervised the study and edited the manuscript. All authors read and approved the final version of the manuscript.

References

1 Evans RL, Faldetta TJ, Humphreys RE, Pratt DM, Yunis EJ, Schlossman SF. Peripheral human T cells sensitized in mixed leukocyte culture synthesize and express Ia-like antigens. *J Exp Med* 1978;148:1440–5.
2 Ko HS, Fu SM, Winchester RJ, Yu DT, Kunkel HG. Ia determinants on stimulated human T lymphocytes. Occurrence on mitogen- and antigen-activated T cells. *J Exp Med* 1979;150:246–55.
3 Oshima S, Eckels DD. Selective signal transduction through the CD3 or CD2 complex is required for class II MHC expression by human T cells. *J Immunol* 1990;145:4018–25.
4 Baecher-Allan C, Wolf E, Hafler DA. MHC class II expression identifies functionally distinct human regulatory T cells. *J Immunol* 2006;176:4622–31.
5 Rea IM, McNerlan SE, Alexander HD. CD69, CD25, and HLA-DR activation antigen expression on CD3+ lymphocytes and relationship to serum TNF-alpha, IFN-gamma, and sIL-2R levels in aging. *Exp Gerontol* 1999;34:79–93.
6 Ferenczi K, Burack L, Pope M, Krueger JG, Austin LM. CD69, HLA-DR and the IL-2R identify persistently activated T cells in psoriasis vulgaris lesional skin: blood and skin comparisons by flow cytometry. *J Autoimmun* 2000;14:63–78.
7 Salgado FJ, Lojo J, Fernandez-Alonso CM, Vinuela J, Cordero OJ, Nogueira M. Interleukin-dependent modulation of HLA-DR expression on CD4 and CD8 activated T cells. *Immunol Cell Biol* 2002;80:138–47.
8 Helft J, Jacquet A, Joncker NT *et al.* Antigen-specific T-T interactions regulate CD4 T-cell expansion. *Blood* 2008;112:1249–58.
9 Mach B, Steimle V, Martinez-Soria E, Reith W. Regulation of MHC class II genes: lessons from a disease. *Annu Rev Immunol* 1996;14:301–31.
10 Holling TM, van der Stoep N, Quinten E, van den Elsen PJ. Activated human T cells accomplish MHC class II expression through T cell-specific occupation of class II transactivator promoter III. *J Immunol* 2002;168:763–70.
11 Gotsman I, Sharpe AH, Lichtman AH. T-cell costimulation and coinhibition in atherosclerosis. *Circ Res* 2008;103:1220–31.
12 Costantino CM, Ploegh HL, Hafler DA. Cathepsin S regulates class II MHC processing in human CD4+ HLA-DR+ T cells. *J Immunol* 2009;183:945–52.
13 Hewitt CR, Feldmann M. Human T cell clones present antigen. *J Immunol* 1989;143:762–9.
14 Costantino CM, Spooner E, Ploegh HL, Hafler DA. Class II MHC self-antigen presentation in human B and T lymphocytes. *PLoS One* 2012;7:e29805.
15 Wong AW, Ghosh N, McKinnon KP *et al.* Regulation and specificity of MHC2TA promoter usage in human primary T lymphocytes and cell line. *J Immunol* 2002;169:3112–9.
16 Steimle V, Otten LA, Zufferey M, Mach B. Complementation cloning of an MHC class II transactivator mutated in hereditary MHC class II deficiency (or bare lymphocyte syndrome). *Cell* 1993;75:135–46.
17 Silacci P, Mottet A, Steimle V, Reith W, Mach B. Developmental extinction of major histocompatibility complex class II gene expression in plasmocytes is mediated by silencing of the transactivator gene CIITA. *J Exp Med* 1994;180:1329–36.
18 van den Elsen PJ, Peijnenburg A, van Eggermond MC, Gobin SJ. Shared regulatory elements in the promoters of MHC class I and class II genes. *Immunol Today* 1998;19:308–12.
19 Harton JA, Ting JP. Class II transactivator: mastering the art of major histocompatibility complex expression. *Mol Cell Biol* 2000;20:6185–94.
20 Chang CH, Hong SC, Hughes CC, Janeway CA Jr, Flavell RA. CIITA activates the expression of MHC class II genes in mouse T cells. *Int Immunol* 1995;7:1515–8.
21 Williams GS, Malin M, Vremec D *et al.* Mice lacking the transcription factor CIITA – a second look. *Int Immunol* 1998;10:1957–67.
22 Arancibia-Carcamo CV, Osawa H, Arnett HA *et al.* A CIITA-independent pathway that promotes expression of endogenous rather than exogenous peptides in immune-privileged sites. *Eur J Immunol* 2004;34:471–80.
23 Arnold PY, Davidian DK, Mannie MD. Antigen presentation by T cells: T cell receptor ligation promotes antigen acquisition from professional antigen-presenting cells. *Eur J Immunol* 1997;27:3198–205.
24 Umeshappa CS, Huang H, Xie Y *et al.* CD4+ Th-APC with acquired peptide/MHC class I and II complexes stimulate type 1 helper CD4+ and central memory CD8+ T cell responses. *J Immunol* 2009;182:193–206.
25 Swartz TJ, Evavold B, Suzuki H, Yokoyama A, Quintans J. Antigenicity of passively acquired major histocompatibility antigens on T cells. *Transplantation* 1988;46:137–43.

26 Tsang JY, Chai JG, Lechler R. Antigen presentation by mouse CD4+ T cells involving acquired MHC class II:peptide complexes: another mechanism to limit clonal expansion? *Blood* 2003;101:2704–10.

27 Nolte-'t Hoen EN, Buschow SI, Anderton SM, Stoorvogel W, Wauben MH. Activated T cells recruit exosomes secreted by dendritic cells via LFA-1. *Blood* 2009;113:1977–81.

28 Patel DM, Arnold PY, White GA, Nardella JP, Mannie MD. Class II MHC/peptide complexes are released from APC and are acquired by T cell responders during specific antigen recognition. *J Immunol* 1999;163:5201–10.

29 Patel DM, Dudek RW, Mannie MD. Intercellular exchange of class II MHC complexes: ultrastructural localization and functional presentation of adsorbed I-A/peptide complexes. *Cell Immunol* 2001;214:21–34.

30 Walker MR, Mannie MD. Acquisition of functional MHC class II/peptide complexes by T cells during thymic development and CNS-directed pathogenesis. *Cell Immunol* 2002;218:13–25.

31 Undale AH, van den Elsen PJ, Celis E. Antigen-independent acquisition of MHC class II molecules by human T lymphocytes. *Int Immunol* 2004;16:1523–33.

32 Game DS, Rogers NJ, Lechler RI. Acquisition of HLA-DR and costimulatory molecules by T cells from allogeneic antigen presenting cells. *Am J Transplant* 2005;5:1614–25.

33 Roederer M. Spectral compensation for flow cytometry: visualization artifacts, limitations, and caveats. *Cytometry* 2001;45:194–205.

34 Beillard E, Pallisgaard N, van der Velden VH *et al.* Evaluation of candidate control genes for diagnosis and residual disease detection in leukemic patients using 'real-time' quantitative reverse-transcriptase polymerase chain reaction (RQ-PCR) – a Europe against cancer program. *Leukemia* 2003;17:2474–86.

35 Tung JW, Heydari K, Tirouvanziam R, Sahaf B, Parks DR, Herzenberg LA. Modern flow cytometry: a practical approach. *Clin Lab Med* 2007;27:453–68, v.

36 Hulspas R, O'Gorman MR, Wood BL, Gratama JW, Sutherland DR. Considerations for the control of background fluorescence in clinical flow cytometry. *Cytometry B Clin Cytom* 2009;76:355–64.

37 Regeczy N, Gorog G, Paloczi K. Developing an expert system for immunophenotypical diagnosis in immunodeficiency. Age-related reference values of peripheral blood lymphocyte subpopulations in Hungary. *Immunol Lett* 2001;77:47–54.

38 Bisset LR, Lung TL, Kaelin M, Ludwig E, Dubs RW. Reference values for peripheral blood lymphocyte phenotypes applicable to the healthy adult population in Switzerland. *Eur J Haematol* 2004;72:203–12.

39 Handunnetthi L, Ramagopalan SV, Ebers GC, Knight JC. Regulation of major histocompatibility complex class II gene expression, genetic variation and disease. *Genes Immun* 2010;11:99–112.

40 Vincent R, Louis P, Gongora C, Papa I, Clot J, Eliaou JF. Quantitative analysis of the expression of the HLA-DRB genes at the transcriptional level by competitive polymerase chain reaction. *J Immunol* 1996;156:603–10.

41 Amlot PL, Tahami F, Chinn D, Rawlings E. Activation antigen expression on human T cells. I. Analysis by two-colour flow cytometry of umbilical cord blood, adult blood and lymphoid tissue. *Clin Exp Immunol* 1996;105:176–82.

42 Fleisher TA. Appendix 2: laboratory reference values. In: Rich RR, Fleisher TA, Shearer WT, Schroeder H, Frew AJ, Weyond CM, eds. *Clinical Immunology: Principles and Practices*. Maryland Heights, MO: Elsevier, 2013:ISBN: 978-0071748896.

43 Herzenberg LA, Tung J, Moore WA, Parks DR. Interpreting flow cytometry data: a guide for the perplexed. *Nat Immunol* 2006;7:681–5.

44 Cheadle WG, Hershman MJ, Wellhausen SR, Polk HC Jr. HLA-DR antigen expression on peripheral blood monocytes correlates with surgical infection. *Am J Surg* 1991;161:639–45.

45 Filion LG, Izaguirre CA, Garber GE, Huebsh L, Aye MT. Detection of surface and cytoplasmic CD4 on blood monocytes from normal and HIV-1 infected individuals. *J Immunol Methods* 1990;135:59–69.

46 Dunham RM, Cervasi B, Brenchley JM *et al.* CD127 and CD25 expression defines CD4+ T cell subsets that are differentially depleted during HIV infection. *J Immunol* 2008;180:5582–92.

47 Peiser M, Becht A, Wanner R. Antibody blocking of MHC II on human activated regulatory T cells abrogates their suppressive potential. *Allergy* 2007;62:773–80.

48 Arruvito L, Payaslian F, Baz P *et al.* Identification and clinical relevance of naturally occurring human CD8+ HLA-DR+ regulatory T cells. *J Immunol* 2014;193:4469–76.

49 Taams LS, van Eden W, Wauben MH. Antigen presentation by T cells versus professional antigen-presenting cells (APC): differential consequences for T cell activation and subsequent T cell-APC interactions. *Eur J Immunol* 1999;29:1543–50.

50 Holling TM, Schooten E, van Den Elsen PJ. Function and regulation of MHC class II molecules in T-lymphocytes: of mice and men. *Hum Immunol* 2004;65:282–90.

51 Wyss-Coray T, Gallati H, Pracht I *et al.* Antigen-presenting human T cells and antigen-presenting B cells induce a similar cytokine profile in specific T cell clones. *Eur J Immunol* 1993;23:3350–7.

52 Lombardi G, Hargreaves R, Sidhu S *et al.* Antigen presentation by T cells inhibits IL-2 production and induces IL-4 release due to altered cognate signals. *J Immunol* 1996;156:2769–75.

53 Sabzevari H, Kantor J, Jaigirdar A *et al.* Acquisition of CD80 (B7-1) by T cells. *J Immunol* 2001;166:2505–13.

54 Tatari-Calderone Z, Semnani RT, Nutman TB, Schlom J, Sabzevari H. Acquisition of CD80 by human T cells at early stages of activation: functional involvement of CD80 acquisition in T cell to T cell interaction. *J Immunol* 2002;169:6162–9.

55 Wetzel SA, McKeithan TW, Parker DC. Peptide-specific intercellular transfer of MHC class II to CD4+ T cells directly from the immunological synapse upon cellular dissociation. *J Immunol* 2005;174:80–9.

56 Hudrisier D, Aucher A, Puaux AL, Bordier C, Joly E. Capture of target cell membrane components via trogocytosis is triggered by a selected set of surface molecules on T or B cells. *J Immunol* 2007;178:3637–47.

57 Davis DM. Intercellular transfer of cell-surface proteins is common and can affect many stages of an immune response. *Nat Rev Immunol* 2007;7:238–43.

58 Rechavi O, Goldstein I, Kloog Y. Intercellular exchange of proteins: the immune cell habit of sharing. *FEBS Lett* 2009;583:1792–9.

59 Gutierrez-Vazquez C, Villarroya-Beltri C, Mittelbrunn M, Sanchez-Madrid F. Transfer of extracellular vesicles during immune cell-cell interactions. *Immunol Rev* 2013;251:125–42.

60 Dhainaut M, Moser M. Regulation of immune reactivity by intercellular transfer. *Front Immunol* 2014;5:112.

61 Revenfeld AL, Baek R, Nielsen MH, Stensballe A, Varming K, Jorgensen M. Diagnostic and prognostic potential of extracellular vesicles in peripheral blood. *Clin Ther* 2014;36:830–46.

Supporting Information

Additional Supporting Information may be found online in the supporting information tab for this article:

Figure S1 Confocal microscopy analysis of HLA-DR mem and HLA-DR IC in $CD4^+$ T cells and $CD19^+$ B cells.